

Growth, thermal, dielectric, linear and nonlinear optical studies of a novel organic single crystal: 2-Amino-5-Chloropyridinium 4-hydroxybenzoate for photonics and nonlinear optical devices

J. Aarthy¹, M. Suriya², K. Sakthi Murugesan³, B. Milton Boaz^{4*}

^{1,2,3,4}Department of Physics, Presidency College, Affiliated to University of Madras, Chennai-600 005, Tamil Nadu India,

*Corresponding Author: miltonboazcm@gmail.com

Available online at: www.isroset.org

Received: 04/Dec/2021, Accepted: 07/Dec/2021, Online: 31/Dec/2021

Abstract— This article deals with the growth and characterization of 2-Amino-5-Chloropyridinium-4-hydroxybenzoate crystals by slow evaporation technique using methanol as solvent. The structural analysis infers the formation of title crystal in to monoclinic system. The various modes of vibrations are detected with suitable FT-IR and FT-Raman peaks. The cut off wavelength of 311 nm and rapid increase in transmission across the visible region assured the transparent nature of the crystal beyond UV region. Further, the broad ultraviolet emission peak centered at 373 nm observed in the photoluminescence analysis strengthen the emission characteristics. In terms of thermal stability, the crystal is stable up to 126 °C with $\leq 10\%$ weight loss and then degrades rapidly. The dielectric parameters depict the usual behavior of the crystal for optical materials. The high work- hardening coefficient 2.38 justifies that the crystal belongs to soft material type. The nonlinear optical characteristics are examined by Z-Scan analysis with an excitation source of 532 nm.

Keywords- Crystal growth, Optical absorption, Thermal analysis, Dielectric measurement, Z-scan studies

I. INTRODUCTION

Organic intermolecular charge-transfer complexes have been extensively studied in the recent past, because of their potential applications in optical data storage systems, nonlinear optics and photoelectric conversion [1-2]. The organic charge-transfer composites consist of delocalized system of donor and acceptor ions. This type of complexes has recently projected in extensive research both theoretically and experimentally [3-5]. Due to their prolonged electric property related to the near molecular packing, organic charge-transfer complexes also found applications in solar cells [6]. Over the recent years, the charge transfer between the aromatic electron acceptors and donors with oxygen, sulphur or nitrogen atoms gained more interest because of their enhanced optical and physicochemical properties. The donor molecule with low ionization ability and the acceptor with excessive ionization potential tend to shape stable inter-molecular charge-transfer complexes [7-9]. The molecule pyridine blended with organic acids and their derivatives are stated to own strong hydrogen-bond interaction and this property plays a considerable role in nonlinear optical properties of materials. In view of this, pyridine-primarily based organic complexes such as 2-amino-5-chloropyridinium-4-aminobenzoate [10], Bis (2-aminopyridinium) maleate [11], 2-aminopyridinium-benzilate [12], 2-amino-5-nitropyridinium-1-tartrate [13], 2-amino-5-bromopyridinium-4-carboxybutanoate

[14] and 2-amino-4-methylpyridinium-3-chlorobenzoate [15] have been extensively studied for their optical and physical properties. Hence in this work, a systematized method was performed to acquire pyridine-primarily based organic NLO crystals which result in the formation of 2-amino-5-chloropyridinium - 4 - hydroxybenzoate crystal. Though the crystal structure of 2-amino -5-choropyridinium -4-hydroxybenzoate has been reported by (Madhukar Hema Malini and Hoong-kun in 2010) yet there is no information available on its detailed growth and characterization for devices. So, attempts are made to grow 2-amino-5-chloropyridinium-4-hydroxybenzoate (2A5C4HB) crystal via a slow evaporation technique using methanol as solvent and obtained successfully.

II. RELATED WORK

Recent years have witnessed the demand of good quality optical crystals for widespread applications in the field of telecommunications, photonic devices, signal processing and optical data storage devices. Pyridine is a heterocyclic compound and their derivative has been widely studied in the past few years in view of their biological, NLO and medical applications. Among the pyridine derivatives, 2-Amino-5-chloropyridine base-acid organic complexes have been extensively studied and reported for their enhanced optical and physical properties. In view of that, the research is developed on the growth of pyridine based organic crystals for nonlinear optical applications. The crystal structure of the title compound 2-Amino-5-chloropyridinium-4-hydroxybenzoate

has been reported by Madhukar Hemamalini and Hoong-Kun in the year 2010. In this present work, to fulfill the need of device application, 2-Amino -5-chloropyridinium -4-hydroxybenzoate organic single crystal was grown to an appreciable size by slow evaporation method. The grown 2-Amino -5-chloropyridinium -4-hydroxybenzoate single crystal was subjected to various characterization studies such as Single crystal X-ray diffraction, spectral, optical, thermal, dielectric, Vickerhardness and Z-scan studies to analyze its suitability for NLO device applications.

III. METHODOLOGY

Materials synthesis and crystal growth

Step I Analytical grades of 2-amino-5-chloropyridine ($C_5H_5ClN_2$) and 4-hydroxy benzoic acid ($C_7H_6O_3$) have been purchased from Avra (98%) and used as received. In the synthesis process, methanol is used as solvent. The growth solution is prepared with 2-amino-5-chloropyridine with 4-hydroxybenzoic acid in the equimolar ratio. The reaction mechanism of the formation 2-amino-5-chloropyridinium-4-hydroxybenzoate is shown in Figure 1.

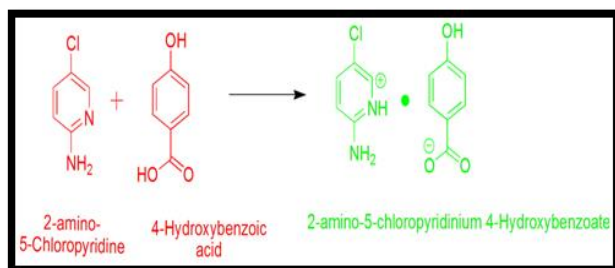


Figure 1. Reaction mechanism of 2A5C4HB crystal.

Step II The experiment is carried out by dissolving the desired quantity of the salts in 50 ml of methanol. Then the solution is left in the stirrer for 7 hours till a homogeneous mixture is attained. Further, the solution is filtered and the residue is preserved in a dust-free environment for 21 days to pursue the crystallization process under optimization condition. At last, a well-grown transparent bulk crystal is acquired, which is displayed in Figure 2.

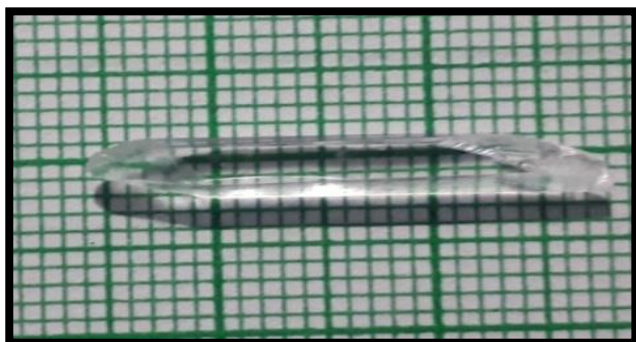


Figure 2. As grown transparent 2A5C4HB crystal.

Characterization tools

The grown crystal is investigated with different characterization techniques for finding its suitability for device applications. The unit cell dimension are

determined using a Bruker Kappa APEX II CCD single crystal X-ray diffractometer with a radiation source of $K\alpha$ with $\lambda = 0.71 \text{ \AA}$. The vibrational properties are examined with PERKIN ELMER FT-IR and FT-RAMAN spectrometer (A BRUKER: RFA 27, 2.0 cm^{-1} resolution). A Perkin Elmer Lambda 950 spectrophotometer is used to obtain a transmittance spectrum in the wavelength range of 200-800 nm. The thermal property is tested by NETZCH STA 409 TGA/DTA analyzer by heating the powdered sample at the rate of 10°C/min across various temperatures ranging from 30 to 450°C . The Jobin-Vyon M/S spectrofluorometer is used to obtain the emissive characteristics of the crystal. The mechanical stability and dielectric nature of the crystal is examined with ECONOMET Vickers hardness tester and HIOKI 3532-50 LCR HITESTER respectively. Finally, the nonlinear optical characteristic is obtained by the Z-scan analysis.

IV. RESULTS AND DISCUSSION

X-ray Diffraction analysis

The structural aspects of the synthesized crystal are determined by using a single-crystal x-ray diffraction experiment. The result of the study reveals that the title crystal belongs to $P2_1/C$ monoclinic space group. The obtained lattice parameters compared with the reported values elsewhere [16] is found to be agrees well. The crystallographic parameters of the crystal are listed in Table 1.

Vibrational analysis

The recorded FT-IR and FT-Raman spectrum of the grown crystal is displayed in Figure 3 and Figure 4 respectively.

Table 1. Crystallographic parameters of the grown 2A5C4HB.

Parameter	Presented study	Reported values
A	10.07 \AA	10.0893 (3) \AA
B	11.81 \AA	11.7612 (4) \AA
C	11.66 \AA	11.6634 (3) \AA
α	90°	90°
β	115°	$116.113 (2)^\circ$
γ	90°	90°
V	1257 \AA^3	$1242.74 (6) \text{ \AA}^3$
Crystal system	Monoclinic	Monoclinic
Space group	$P2_1/c$	$P2_1/c$

The functional group vibrations present in the spectrum assured the formation of 2-amino-5-chloropyridinium-4-

hydroxybenzoate. The different modes of vibrations and possible assignments are listed in the Table 2.

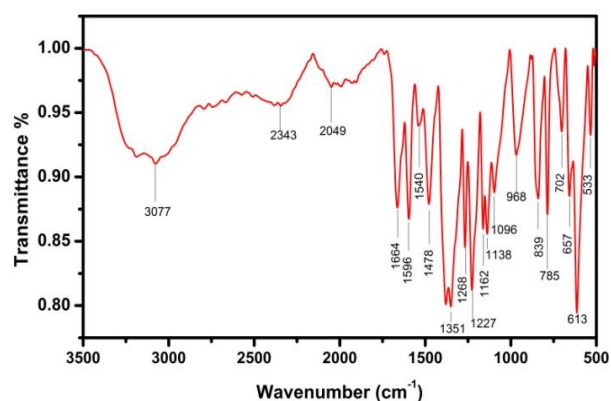


Figure 3. FT- IR spectrum of 2A5C4HB crystal.

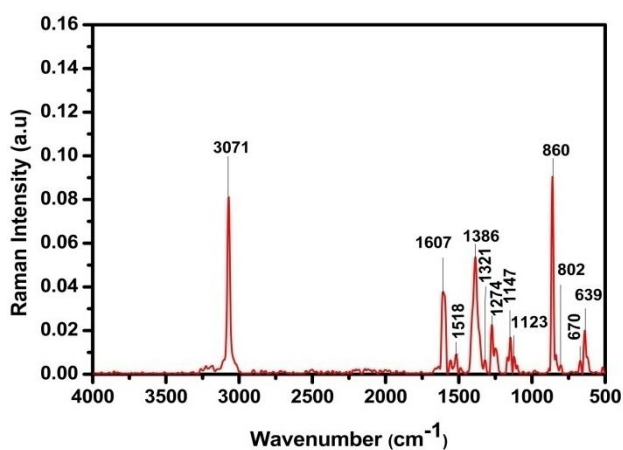


Figure 4. FT- Raman spectrum of 2A5C4HB crystal.

Table 2. FT-IR and FT-Raman frequency assignments of 2A5C4HB crystal.

IR frequency (cm ⁻¹)	Raman frequency (cm ⁻¹)	Assignments
3077	3072	C – H stretching vibration of pyridinium ring
1664	-	Alkenyl group of C = C stretching vibration
1596	1607	C = C stretching vibration
-	1556	N – H bending vibration
1540	1518	N – O stretching vibration
1478	-	C = N stretching vibration
1351	1321	In-plane bending of O – H group

1268	1274	C – N stretching vibration of primary amine
1227	1250	C – O stretching vibration
1162	1147	C – N stretching vibration of secondary amine group
1096	-	C – H in-plane bending vibration
839	670	C – H out-of-plane bending vibration
785	-	C – Cl stretching vibration
657	-	Alkyne group of C – H bending vibration

Carbon-Hydrogen mode of interactions

The first IR vibration observed at 657 cm⁻¹ is assigned to C-H bending vibrations. The aromatic C-H out of plane bending is seen at 839 cm⁻¹ and 670 cm⁻¹ in the FT-IR and FT Raman spectrum respectively. Then, a C-H in-plane bending is identified at 1096 cm⁻¹ in FT-IR spectrum. Finally, the stretching vibrations are evident at 3077 cm⁻¹ and 3072 cm⁻¹ in the FT-IR and FT-Raman spectrum respectively.

Carbon=Carbon and Carbon=Nitrogen mode of interactions

The carbon-nitrogen (C=N) interactions are detected in the FTIR spectra at 1478 cm⁻¹. The aromatic C=C mode of assignments are observed at 1596 cm⁻¹ (IR) and 1607 cm⁻¹ (Raman) respectively. Further, the alkenyl C=C stretching IR vibration is seen at 1664 cm⁻¹.

Carbon-Oxygen, Nitrogen-Oxygen and Oxygen-Hydrogen mode of interactions

The carboxylate group C-O stretching is observed in both FTIR and Raman spectrum at 1227 cm⁻¹ and 1250 cm⁻¹, respectively. Similarly, the nitrogen-oxygen bond stretching of IR and Raman vibrations are seen at 1540 cm⁻¹ and 1518 cm⁻¹ respectively. The O-H group in-plane bending is observed at 1351 cm⁻¹ and 1321 cm⁻¹ in FTIR and Raman spectrum respectively.

Carbon-Nitrogen Stretching and Nitrogen-Hydrogen mode of interactions

The secondary amine group C-N stretching vibration peak is observed at 1162 cm⁻¹ in the FT-IR spectrum and 1147 cm⁻¹ in the FT-Raman spectrum. The aromatic primary amine group of C-N stretching vibration peak is detected in the FT-IR spectrum at 1268 cm⁻¹ and in the FT-Raman spectrum at 1274 cm⁻¹. In the FT-Raman spectrum, the N-H bending vibration of secondary amine is observed at 1556 cm⁻¹.

Carbon-Chlorine vibration

The C-Cl stretching vibration of pyridinium ring is confirmed with an intense absorption peak at 785 cm^{-1} in the FTIR spectrum.

Linear optical analysis

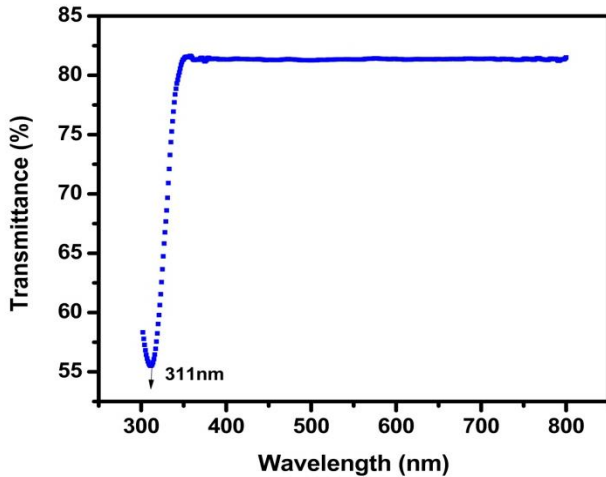


Figure 5. UV-Vis-NIR transmission spectra of 2A5C4HB crystal.

The recorded UV-Vis-NIR transmission spectrum for the synthesized crystal in the 200-800 nm wavelength regions is displayed in Figure 5. In the case of NLO crystals, high transmittance with a low cut off wavelength ($\lambda_{\text{cut-off}}$) is desired for potential applications [17]. Examination of the spectrum reveals that in the present crystal, the cut-off wavelength ($\lambda_{\text{cut-off}}$) is observed at 311 nm with increase in transparent nature across the visible region of the spectrum. The crystal has a significant rise in transmission beyond the cut-off wavelength and becomes nearly transparent ($\geq 80\%$) in the visible region. It denotes the non-absorbing nature of the title crystal beyond the mid UV region. These are the desirable property for the materials used in NLO applications. To obtain the optical band gap, the absorption coefficient in other words, alpha is determined by using the following relation as reported elsewhere [18].

$$\alpha = \frac{2.303 \times \log(\frac{1}{T})}{t} \quad (1)$$

Then, the optical band gap is calculated by tauc relation

$$(\alpha h\nu) = A(E_g - h\nu)^n \quad (2)$$

Where, T is the transmittance, t is the thickness, h is the Planck's constant, ν is the frequency and A is a constant. The value of n is a variable that takes $\frac{1}{2}$ for direct allowed transition and 2 for indirect permitted transitions. In this case, the crystal belongs to direct transition classes; the graph is plotted with photon energy along the x-axis versus $(\alpha h\nu)^2$ along the y-axis. The extrapolation of the plot at $x=0$ gives the optical band gap of the title crystal as shown in Figure 6. In the theoretical aspect, the cut-off

wavelength (λ_{cutoff}) 311 nm is utilized to obtain the optical band gap by using Planck's equation ($E = h\nu$). The experimental band gap of 4.12 eV determined from the graph is nearly coinciding with the theoretical value 3.99 eV. Overall, a desired low cut-off wavelength and transparent nature in the visible region make this material highly suitable for UV-light-driven applications.

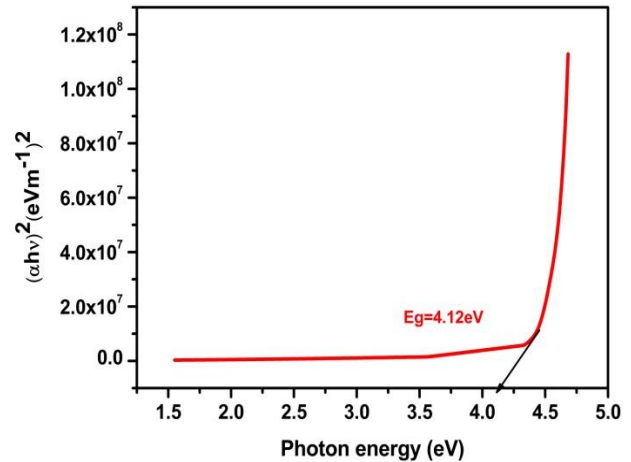


Figure 6. Tauc Plot of 2A5C4HB crystal.

Thermal analysis

Thermal analysis is a popular method for investigating the thermo physical and kinetic properties of materials [19-20]. The TG-DTA spectrum of the title crystal is depicted in Figure 7. The TG graph demonstrates that the title crystal was stable till $126\text{ }^\circ\text{C}$ and then, the decomposition occurs in a single stage weight loss. The breakdown occurred between $126\text{ }^\circ\text{C}$ and $247\text{ }^\circ\text{C}$, indicates that 99.7 percent of the substance being eliminated as gaseous products. The DTA curve of the grown crystal reveals a sharp peak at $211\text{ }^\circ\text{C}$ due to endothermic reactions which predicts the melting point of the crystal. Also, the sharp peak replicates the crystal's purity. Thus, the 2A5C4HB crystal has shown promising signs for device applications which works under $126\text{ }^\circ\text{C}$. The thermal stability of the title crystal is compared with other prominent nonlinear optical crystals and listed in Table 3.

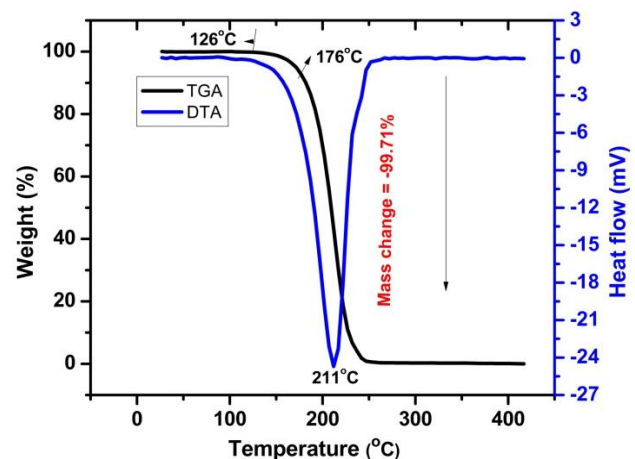


Figure 7. TG/DTA curves of 2A5C4HB crystal.

Table 3. Thermal stability of present crystal in comparison with other nonlinear crystals.

Compounds	Thermal stability (°C)	Reference
Guanidiniummaganesesulphate hydrate	73	[21]
2-Amino 4,6-dimethyl pyrimidine-4- nitrophenol	120	[22]
L-alanine-2-furoic acid	122	[23]
LAT	118	[24]
2-Amino-5-chloropyridinium-2,4-dinitrophenolate	122	[25]
2-Amino-5-chloropyridine	109.85	[26]
2-Amino-5-chloropyridinium-4-hydroxybenzoate	126	Present work

Dielectric studies

The dielectric analysis gives vital information about the nature of atoms, ion, and their bonding nature of materials [27-28]. In the present case, the dielectric measurement is carried out on the crystal with dimensions of 11×6×1.73 mm³ over 50 Hz to 5 MHz frequency at variable temperatures. The dielectric constant and dielectric loss of the 2A5C4HB crystal can be estimated by the following expressions.

$$\epsilon' = \frac{C_p d}{A \epsilon_0} \tag{3}$$

$$\epsilon'' = \epsilon' \tan \delta \tag{4}$$

Where ‘C_p’ is the parallel capacitance, ‘ε₀’ is the absolute permittivity at free space (8.854×10⁻¹² Fm⁻¹), ‘d’ is the crystal’s thickness and tan δ is the dissipation factor. The obtained ε’ and ε’’ are plotted against frequency as depicted in Figure 8 and Figure 9 respectively. Both the values have shown high values in the low-frequency range and lower values in the higher frequency region. The former may be attributed to the existence of all four polarizations and the latter implies the good optical quality of the crystal with fewer imperfections. Overall, the grown crystal shows promising signs for nonlinear optical applications.

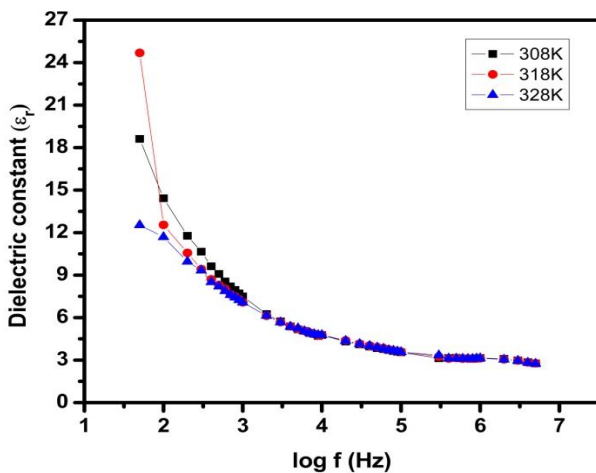


Figure 8. The plot of log f vs dielectric constant of 2A5C4HB crystal.

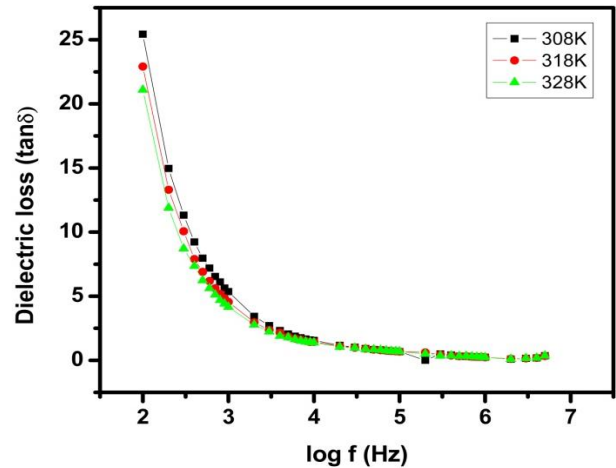


Figure 9. The plot of log f vs dielectric loss of 2A5C4HB crystal.

Microhardness measurements

The microhardness testing of a single crystal is essential to understand the various material characteristics and its subsequent impressions made in the surface [29]. The indentations were made with various loads at the time interval of 10s during the experiment. The hardness number is given by the expression,

$$H_V = 1.8544 \left(\frac{P}{d^2} \right) \tag{5}$$

Where, P is the applied load (kgs) and d is the diagonal length of the indentation in millimeters. The variation of microhardness with the function of load is plotted as shown in Figure 10.

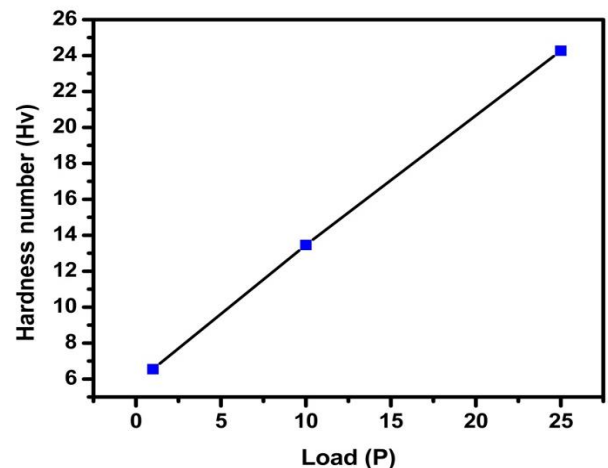


Figure 10. Plot of Hardness number vs variable load.

The analysis revealed the increasing hardness value for increasing load and attributed it to the surface layer’s work hardening. When the applied load goes beyond 25 g, the fracture in the surface is enhanced around the indentation mark implying the liberation of interior stresses [30]. Figure 11 depicts the graph plotted for Log (p) vs. Log (d) and the slope of the curve defines the work hardening coefficient ‘n.’ According to Onitsch, the materials are

categorized into hard material and soft materials with the values of $n \leq 1.6$ and $n \geq 1.6$ respectively [31]. The n value of the 2A5C4HB crystal is 2.38 identifies the soft material nature of the crystal.

Estimation of solid-state parameters

The electronic polarizability (α) was calculated using a dielectric constant at higher frequencies. To understand the material property further, few other solid state parameters have to be determined for the crystal. At first, the density of the 2A5C4HB crystal is calculated by using the relation

$$\rho = \frac{MZ}{N_a V} \tag{6}$$

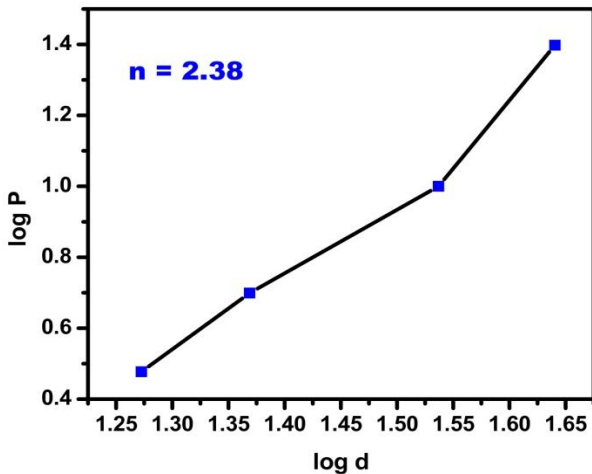


Figure 11. Log (p) versus Log (d) of 2A5C4HB.

Where M – Molecular weight (266.68 g/mol), Z - Number of molecules in the unit cell ($Z=4$ in our case), N_a – Avogadro’s number ($6.203 \times 10^{23} \text{ mol}^{-1}$) and V - Volume of the unit cell. The estimated density of 1.42 Mg/m^3 agrees with the one estimated with the single crystal XRD measurements [16]. Further, the valence electron plasma energy ($\hbar\omega_p$) is 14.46 eV estimated as by the relation reported elsewhere [32].

$$\hbar\omega_p = 28.8 \sqrt{\frac{Z\rho}{M_w}} \tag{7}$$

The obtained value is utilized to determine the Penn gap (E_p) and Fermi gap (E_f) of the title crystal in terms of plasma energy by using the relations [33-34]

$$E_p = \frac{(\hbar\omega_p)}{(\epsilon_r - 1)^{\frac{1}{2}}} \tag{8}$$

$$E_f = 0.2948(\hbar\omega_p)^{\frac{4}{3}} \tag{9}$$

Where $\epsilon_r = 24.7$ is the maximum value of the dielectric constant of the material. The estimated values of E_p and E_f are found to be 2.97 and 10.38, respectively. Finally, the most desired value the electronic polarizability (α) of the 2A5C4HB crystal was calculated by using the relation,

$$\alpha = \frac{0.396M}{\rho} \left[\frac{(\hbar\omega_p)^2 S_0}{(\hbar\omega_p)^2 S_0 + 3E_p^2} \right] \times 10^{-24} \text{ cm}^3 \tag{10}$$

Where, S_0 is the constant and which is obtained by

$$S_0 = 1 - \left[\frac{E_p}{4E_f} \right] + \frac{1}{3} \left[\frac{E_p}{4E_f} \right]^2 \tag{11}$$

The calculated value of the constant $S_0 = 0.9302$ and the determined value of (α) is $6.5230 \times 10^{-23} \text{ cm}^3$ respectively. For further validation, Clausius-Mossotti relation is used and the following equation estimates the value of $6.5884 \times 10^{-23} \text{ cm}^3$.

$$\alpha = \frac{3M}{4\pi N_a \rho} \left[\frac{\epsilon_r - 1}{\epsilon_r + 2} \right] \text{ cm}^3 \tag{12}$$

Table 4 represents the various estimated values of the title crystal is displayed for reference in table 4. Apart from the Penn gap perspective, in terms of optical band gap relations, the following expression may also used to estimates the electronic polarizability

$$\alpha = 0.396 \left[1 - \frac{\sqrt{E_g}}{4.06} \right] \frac{M}{\rho} \times 10^{-24} \text{ cm}^3 \tag{13}$$

Table 4. Calculated solid-state parameters of the grown 2A5C4HB crystal

Parameters	Values
Crystal density (ρ)	1.4259 Mg/m ³ (Theoretical) 1.425 Mg/m ³ (Experimental)
Plasma energy ($\hbar\omega_p$)	14.4658 (eV)
Penn gap energy (E_p)	2.9714 (eV)
Fermi energy (E_f)	10.3815 (eV)
Specific material constant (S_0)	0.9302
Penn analysis (α_p)	$6.5230 \times 10^{-23} (\text{cm}^3)$
Clausius-Mossotti (α_c)	$6.5884 \times 10^{-23} (\text{cm}^3)$
optical band gap value (α_o)	$3.7061 \times 10^{-23} (\text{cm}^3)$

Photoluminescence analysis

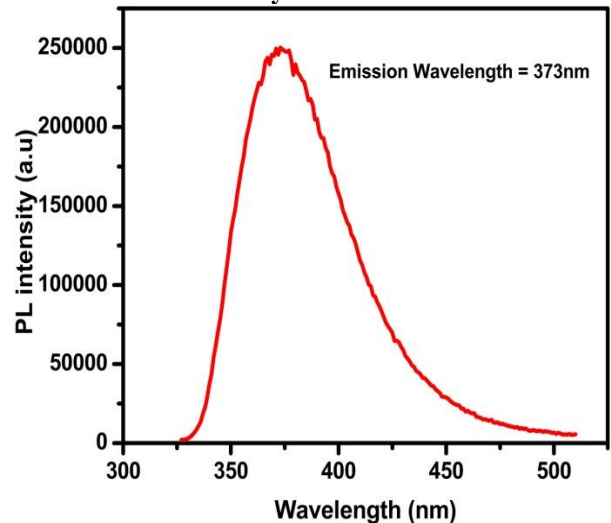


Figure 12. Photoluminescence spectrum of 2A5C4HB crystal.

The emission behavior is examined by exciting the title crystal at 270 nm and documented at room temperature across the 250-500 nm region of the EM spectrum. The PL emission spectrum as shown in Figure 12 has displayed a strong emission peak with maxima centered at 373 nm confirming an ultraviolet emission. Thus, the title crystal extends its application in ultraviolet light-based LED and other optical device applications [35].

Third Harmonic generation studies

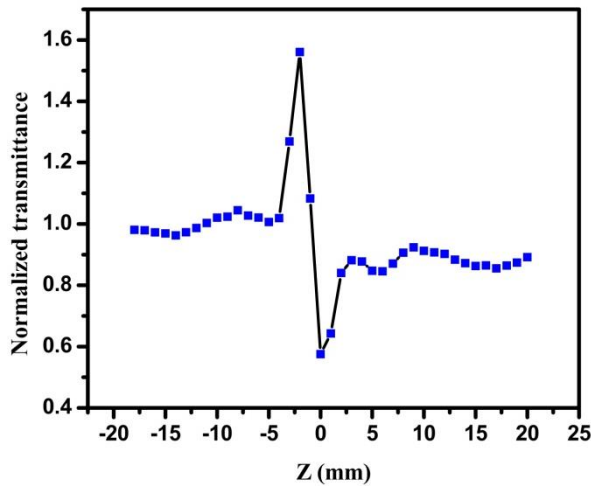


Figure 13. Closed aperture curves of 2A5C4HB crystal.

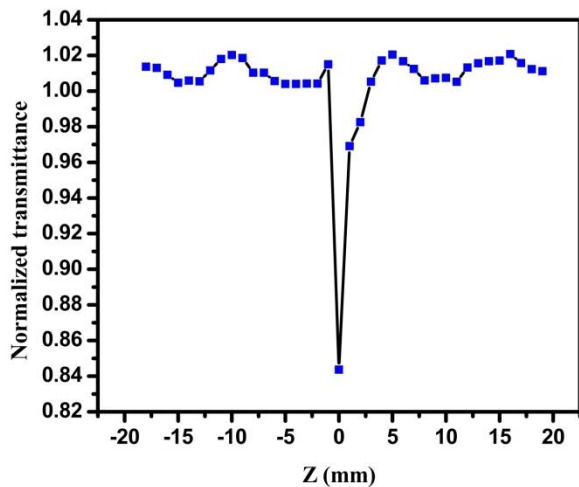


Figure 14. Open aperture curve of 2A5C4HB crystal.

The Z-Scan method is a popular experimental tool to evaluate the nonlinear characteristics of semiconductors [36-37], dielectrics [38-41], organic or carbon-based molecules [42] and liquid crystals [43] respectively. It enables the calculation of the essential parameters of photonic applications such as non-linear refractive index and non-linear absorption coefficient by using closed and open methods [44-46]. The closed and open aperture Z-scan plots of the 2A5C4HB crystal is shown in Figure 13 and 14 respectively. The crystal's self-defocusing effect is a crucial property related to the local deviation of the refractive index with temperature is used in the field of optical sensor applications [47-48]. The influence of

negative nonlinearity, i.e., a high self-defocusing refractive index effect, is seen by the sharp peak followed by a valley-normalized transmittance peak obtained from closed aperture Z-scan data [49-50].

The open aperture transmittance data is utilized to determine various parameters. The following relation gives the aperture linear transmittance (S)

$$S = 1 - \exp(-2 \frac{r_a^2}{\omega_a^2}) \tag{14}$$

The obtained S value is substituted in the following relation to estimate the deviation in peak-valley transmittance (ΔT_{p-v}) by

$$\Delta T_{p-v} = 0.406(1 - S)^{0.25} |\Delta \phi| \tag{15}$$

Where, r_a and ω_a is the aperture and beam radius respectively. Then, the linear absorption (α) and the thickness of the crystal (L) in the following equations give the effective length of the crystal (L_{eff})

$$L_{eff} = \frac{[1 - \exp(-\alpha L)]}{\alpha} \tag{16}$$

The substitution of these known values in the following expression gives the nonlinear refractive index of the 2A5C4HB crystal

$$n_2 = \frac{\Delta \phi}{K I_0 L_{eff}} \tag{17}$$

Where, I_0 is the laser beams intensity at origin and $K = 2\pi/\lambda$ ($\lambda = 532$ nm). The following expression is used to determine the nonlinear absorption coefficient

$$\beta = \frac{2\sqrt{2}\Delta T}{I_0 L_{eff}} \tag{18}$$

Where, ΔT denotes the value of one valley obtained from the open aperture curve. The β value lies in the negative scale for saturable absorption and changes to positive for two-photon absorptions. The following expression gives the real part and imaginary components of the nonlinear optical susceptibility (χ^3)

$$R_e \chi^3 (esu) = 10^{-4} \left(\frac{\epsilon_0 C^2 n_0^2 n^2}{\pi} \right) \left(\frac{cm^2}{W} \right) \tag{19}$$

$$I_m \chi^3 (esu) = 10^{-2} \left(\frac{\epsilon_0 C^2 n_0^2 \lambda \beta}{4\pi^2} \right) \left(\frac{cm}{W} \right) \tag{20}$$

Where, ϵ_0 is permittivity in a vacuum, C is the velocity of light and n_0 is the linear refractive index respectively. The absolute value of χ^3 is determined by using the relation,

$$\chi^3 = [\sqrt{(R_e \chi^3)^2 + (I_m \chi^3)^2}]^{\frac{1}{2}} \tag{21}$$

The Z scan experimental details and the obtained results are summarized in Table 5. The obtained values of the

2A5C4HB crystal identify them as a suitable candidate in the fabrication of non-linear optical devices.

Table 5. Experimental and obtained results of the Z-scan analysis

Focal length of the lens used	103 mm
Optical path length	700 mm
Beam radius of the aperture (ω_a)	3.5 mm
Aperture radius (r_a)	1.25 mm
Sample thickness (l)	1 mm
Beam radius (ω_L)	3.1 mm
Nonlinear refractive index (n_2)	$1.3726 \times 10^{-9} \text{ cm}^2/\text{W}$
Nonlinear absorption coefficient (β)	$3.1371 \times 10^{-4} \text{ cm/W}$
Real part of the third-order susceptibility [$\text{Re}(\chi^3)$]	$5.2139 \times 10^{-7} \text{ esu}$
Imaginary part of the third order susceptibility [$\text{Im}(\chi^3)$]	$2.0255 \times 10^{-7} \text{ esu}$
Third-order susceptibility (χ^3)	$5.59 \times 10^{-7} \text{ esu}$

V. CONCLUSION

2-amino-5-chloropyridinium-4-hydroxybenzoate single crystal was successfully grown at room temperature with methanol as a solvent. A monoclinic crystal structure of the compound with the space group P21/c was validated by XRD analysis. The FTIR and FT-RAMAN investigation disclosed all the characteristics of functional groups of the produced 2A5C4HB crystal. The optical transmittance spectrum shows the cut-off wavelength of the crystal at 311 nm and 81 percent transparency in the whole visible domain. The photoluminescence spectrum reveals that the crystal has a broad ultraviolet emission peak at 373 nm. According to thermo gravimetric measurements, the crystal is thermally stable up to 126 °C without any significant weight loss. The results of dielectric studies on the 2A5C4HB crystal exhibit normal behavior with high optical quality and confirm its application in the microelectronic industry. Micro-hardness tests revealed the soft material nature of the crystal. Z-scan experiments inferred the saturable absorption and self-defocusing nature of the 2A5C4HB crystal. All the preceding results indicate that the grown 2-amino-5-chloropyridinium-4-hydroxybenzoate crystal can be used to fabricate a variety of nonlinear optical and photonic devices.

ACKNOWLEDGMENT

The authors thank the authorities of SAIF, IIT Madras, Chennai-36 for completing the characterization such as Single Crystal XRD, FT-IR, FT-RAMAN and Thermal measurements.

REFERENCES

- [1] J. Ulanski, "Conductivity of organic composites with 3- and 2-dimensional crystalline networks I. Continuity of the conducting phase", *Synthetic Metals*, Vol. **39**, Issue. **1**, pp. **13-24**, **1990**.
- [2] Toshikazu Ono, "Inclusion Crystal Growth and Optical Properties Of Organic Charge-Transfer Complexes Built from Small Aromatic Guest Molecules and Naphthalenediimide Derivatives", *Chemistry Letters*, Vol. **46**, Issue. **6**, pp. **801-804**, **2017**.
- [3] Amparo Salmerón-Valverde and Sylvain Bernès, "Crystal growth and characterization of solvated organic charge-transfer complexes built on TTF and 9-dicyanomethylene fluorene derivatives", *CrystEngComm*, Vol. **17**, Issue. **32**, pp. **6227-6235**, **2015**.
- [4] R. Bharathikannan, A. Chandramohan, M. A. Kandhaswamy, J. Chandrasekaran, R. Renganathan and V. Kandavelu, "Synthesis, crystal growth and properties of the charge transfer complex adduct of 2-nitro aniline with picric acid – An organic non-linear optical material", *Cryst. Res. Technol*, Vol. **43**, Issue. **6**, pp. **683-688**, **2008**.
- [5] M. Amudha, R. Rajkumar, V. Thayanithi and P. Praveen Kumar, "Growth and Characterization of Benzimidazolium Salicylate: NLO Property from a Centrosymmetric Crystal", *Advances in Optical Technologies*, Vol. **19**, Issue. **10**, pp. **9-10**, **2015**.
- [6] A. Chandramohan, R. Bharathikannan, J. Chandrasekaran, P. Maadeswaran, R. Renganathan and V. Kandavelu, "Synthesis, crystal growth and characterization of a new organic NLO material: Caffeinium picrate (CAFP)—A charge transfer molecular complex salt", *Journal of Crystal Growth*, Vol. **310**, Issue. **32**, pp. **5409-5415**, **2008**.
- [7] Alexander Eychmüller and Andrey L. Rogach, "Chemistry and photophysics of thiol-stabilized II-VI semiconductor nanocrystals", *Pure Appl. Chem*, Vol. **72**, Issue. **1-2**, pp. **179-188**, **2000**.
- [8] Hassan S. Bazzi, Adel Mostafa, Siham Y. AlQaradawi and El-Metwally Nour, "Synthesis and spectroscopic structural investigations of the charge-transfer complexes formed in the reaction of 2, 6-diaminopyridine with -acceptors TCNE, chloranil, and DDQ", *Journal of molecular structure*, Vol. **842**, Issue. **1-3**, pp. **1-5**, **2007**.
- [9] Zdzisław Latajka, Grzegorz Gajewski, Austin J. Barnes, Dongfeng Xue and Henryk Ratajczak, "Hyperpolarizabilities of some model hydrogen-bonded complexes: PM3 and ab initio studies", *Journal of molecular structure*, Vol. **928**, Issue. **1-3**, pp. **121-124**, **2009**.
- [10] M. Krishnakumar, K. Thirupugalmani and S. Brahadesewaran, "Studies on structure, growth and characterization of third order nonlinear optical 2-amino-5-chloropyridinium-4-amino benzoate single crystal", *Materials Science-Poland*, Vol. **35**, Issue. **2**, pp. **313-321**, **2017**.
- [11] P.V. Dhanaraj, N.P. Rajesh and G. Bhagavannarayan, "Synthesis, crystal growth and characterization of an organic NLO material: Bis(2-aminopyridinium) maleate", *Physica B*, Vol. **405**, Issue. **16**, pp. **3441-3445**, **2010**.
- [12] S. Madhankumar, P. Muthuraja and M. Dhandapani, "Structural characterization, quantum chemical calculations and Hirshfeld surface analysis of a new third order harmonic organic crystal: 2-Amino-4-methylpyridinium benzilate", *Journal of Molecular structure*, Vol. **1201**, Issue. **1-2**, pp. **127151-127152**, **2020**.
- [13] S. Manikandan and S. Dhanuskodi, "EPR of -irradiated single crystals of 2-amino-5-nitro pyridinium l-tartrate: A NLO material", *Spectrochimica Acta Part A*, Vol. **67**, Issue. **1**, pp. **160-165**, **2007**.
- [14] S. Vasuki, R. T. Karunakaran and G. Shanmugam, "Growth and physicochemical studies on 2-amino 5-bromopyridinium 4-carboxybutanoate: an organic NLO single crystal", *J Mater Sci: Mater Electron*, Vol. **28**, Issue. **17**, pp. **12916-12928**, **2017**.
- [15] B. Babu, J. Chandrasekaran, R. Thirumurugan, K. Anitha and M. Saravanabhavan, "2-Amino 4-methylpyridinium 3-chlorobenzoate A phase matchable organic nonlinear optical

- material for optoelectronics device applications”, Optics and Laser Technology, Vol. **94**, Issue. **1**, pp. **253-260**, **2017**.
- [16] Madhukar Hemamalini and Hoong-Kun Fun, “2-Amino-5-chloropyridinium 4-hydroxybenzoate”, Acta Crystallographica Section E, Vol. **E66** pp. **0557**, **2010**.
- [17] S.Chidambaram, A.David Kalaimani Raj, R.Punniyamoorthy and R.Manimekalai, “Growth and characterization of Strontium Chloride added Nicotinic Acid Single Crystals”, International Journal of Scientific Research in Physics and Applied Sciences, Vol. **6**, Issue. **4**, pp. **39-43**, **2018**.
- [18] T.Jayanalina, G.Rajarajan, K.Boopathi and K.Sreevani, “Synthesis, growth, structural, optical and thermal properties of a new organic nonlinear optical crystal: 2- amino 5- chloropyridinium-L-tartrate”, Journal of Crystal Growth, Vol. **426**, Issue. **1**, pp. **9-14**, **2015**.
- [19] A.S. Haja Hameed, G. Ravi, R. Dhanasekaran and P. Ramasamy, “Studies on organic indole-3-aldehyde single crystals”, Journal of Crystal Growth, Vol. **212**, Issue. **1-2**, pp. **227-232**, **2000**.
- [20] Suthan, N.P. Rajesh, C.K. Mahadevan and G. Bhagavannarayan, “Studies on crystal growth and physical properties of 2-amino-5-chloropyridine single crystal”, Materials Chemistry and Physics, Vol. **129**, Issue. **1-2**, pp. **433-438**, **2011**.
- [21] A. Rajeswari, G. Vinita and P. Murugakoothan, “Investigation on optical, thermal, mechanical, dielectric and ferroelectric properties of non linear optical single crystal guanidinium manganese sulphate”, J. Mater. Sci. Mater Electron, Vol. **29**, Issue. **1**, pp. **12526-12535**, **2018**.
- [22] P. Karuppasamy, T. Kamalesh, K. Anitha, S. Abdul Kalam, Muthusenthilpandian, P.Ramasamy, Sunilverma and S.VenugopalRao, “Synthesis, Crystal growth, structure and characterization of a novel third order nonlinear optical organic single crystal: 2-amino-4,6-Dimethyl Pyrimidine 4- nitrophenol”, Optical materials, Vol. **84**, Issue. **1**, pp. **475-489**, **2018**.
- [23] B. Uma, R. Samuel Selvaraj, S. Krishnan and B. Milton Boaz, “Growth and characterization of a novel organic nonlinear optical material: l-alanine 2-furoic acid”, Optik, Vol. **125**, Issue. **2**, pp. **651-656**, **2014**.
- [24] M. Vimalan, T. Rajesh Kumar, S. Tamilselvan, P. Sagayaraj and C.K. Mahadevan, “Growth and properties of novel organic nonlinear optical crystal: l-aluminium tartrate (LAT)”, Phys. B, Vol. **405**, Issue. **18**, pp. **3907-3913**, **2010**.
- [25] Pullithodi Mohamed Kutty, Joseph Chandrasekaran, Balraj Babu and Yoshitaka Matsushita, “Spectroscopic Investigations on New Organic NLO crystal – 2-amino-5- chloropyridinium-2,4-dinitrophenolate”, Z. Phys. Chem, Vol. **232**, Issue. **1**, pp. **802**, **2017**.
- [26] Suthan, N.P. Rajesh, C.K. Mahadevan and G. Bhagavannarayanan, “Studies on crystal growth and physical properties of 2-amino-5-chloropyridine single crystal”, Materials chemistry and physics, Vol. **129**, Issue. **1**, pp. **433-438**, **2015**.
- [27] Suresh Sagadevan and Priya Murugasen, “Optical and Dielectric Studies on semi organic nonlinear optical crystal by solution growth technique”, International Journal of Recent advances in Physics, Vol. **3**, Issue. **1**, pp. **123-125**, **2014**.
- [28] Varghese Mathew, Sabu Jacob, C.K. Mahadevan and K.E. Abraham, “A study of thermal, dielectric and magnetic properties of strontium malonate crystals”, Physica B, Vol. **407**, Issue. **2**, pp. **222-226**, **2012**.
- [29] T. Suthan, N.P. Rajesha, C.K. Mahadevan, K. Senthil Kumar and G. Bhagavannarayan, “Growth and characterization of organic material 2-methylamino-5-chlorobenzophenone single crystal by modified vertical Bridgman technique”, Spectrochimica Acta Part A, Vol. **79** Issue. **5**, pp. **1443-1448**, **2011**.
- [30] E. M. Onitsch, “The present status of testing the hardness of materials”, Mikroskopie, Vol. **95**, pp. **12-14**, **1956**.
- [31] Sudeshna Mukerji and Tanusree Kar, “Etch pit study of different crystallographic faces of L-arginine hydrobromide monohydrate (LAHBr) in some organic acids”, Journal of Crystal Growth, Vol. **204**, Issue. **3**, pp. **341-347**, **1999**.
- [32] J.D. Jackson, “Classical Electrodynamics, 2nd edn”, Wiley Eastern Limited, New York, pp. **156-160**, **1978**.
- [33] Ravindra NM, Bharadwaj RP, Sunil Kumar K and Srivastava VK, “Model based studies of some optical and electronic properties of narrow and wide gap materials”, Infrar Phys, Vol. **21**, Issue. **6**, pp. **369-381**, **1981**.
- [34] Penn DR, “Wave-number-dependent dielectric function of semiconductors”, Phys Rev, Vol. **128**, Issue. **5**, pp. **2093-2097**, **1962**.
- [35] Rezaq Naji Aljawfi, Moh. Jane Alam, F. Rahman, Shabbir Ahmad, Aga Shahee and Shalendra Kumar, “Impact of annealing on the structural and optical properties of ZnO nanoparticles and tracing the formation of clusters via DFT calculation”, Arabian Journal of Chemistry, Vol. **13**, Issue. **1**, pp. **2207-2218**, **2020**.
- [36] Sheik-Bahae. M, Said. AA, Wei. TH, Hagan. DJ and Stryland. EV, “Sensitive measurement of optical nonlinearities using a single beam”, IEEE J. Quantum Electron, Vol. **26**, pp. **760-769**, **1990**.
- [37] Zhao. W and Palffy-Muhoray, “Z- scan technique using top-hat beams”, Appl.Phys.Lett, Vol. **63**, Issue. **12**, pp. **1613**, **1993**.
- [38] Desouza. PC, Nader. G, Catunda. T, Muramatsu. M and Horowicz. RJ, “Application of the Z-scan technique to a saturable photorefractive medium with the overlapped ground and excited state absorption”, Opt. Comm, Vol. **177**, Issue. **1-6**, pp. **417-423**, **1999**.
- [39] Kobayashi. T, “nonlinear optics of organics and semiconductors”, nonlinear optics- Springer - Verlag, Berlin, pp. **131-135**, **1991**.
- [40] Shirk. JS, Pong. RGS, Bartoli. FJ and Snow. AW, “Optical limiter using a lead Phthalocyanine”, Appl.Phys.Lett, Vol. **63**, Issue. **14**, pp. **1880**, **1993**.
- [41] Ditlbacher. H, Krenn. JR, Lamprecht. B, Leitner. A and Aussenegg. FR, “Spectrally coded optical data storage by metal nanoparticles”, Opt. Lett, Vol. **25**, Issue. **8**, pp. **563**, **2000**.
- [42] Gannev. RA, “Nonlinear refraction and nonlinear absorption of various media”, J. Opt. A: pure and App. Opt, Vol. **7**, Issue. **1**, pp. **717-733**, **2005**.
- [43] Krauss D Todd and Wise W Frank, “Femtosecond measurements of nonlinear absorption and refraction in CdS, ZnSe, and ZnS”, Appl. Phys. Lett, Vol. **65**, Issue. **14**, pp. **1739**, **1994**.
- [44] Ma. H, Gomes. SL and Cid B de Arajo, “Infrared nonlinearity of commercial Cd (S,Se) glass composites”, Opt.Comm, Vol. **87**, Issue. **1-2**, pp. **19-22**, **1992**.
- [45] Rangel – Rojo. R, Kosa. T, Hajto. E, Eswen. PJS, Owen. AE, Kar. AK and Wherrett. BS, “Near – infrared optical nonlinearities in amorphous chalcogenides”, Opt.Comm, Vol. **109**, Issue. **1-2**, pp. **145-150**, **1994**.
- [46] Wei. TH, Hagan. DJ, Sence. MJ, VanStryland. EW, Perry. JW and Coulter. DR, “Direct measurements of nonlinear absorption and refraction in solutions of phthalocyanines”, Appl. Phys. B, Vol. **54**, Issue. **6**, pp. **46-51**, **1992**.
- [47] PApora. D, Maddalena. P, Abbade. G, Santamoto. E and Jannossy, “Wavelength dependence of optical reorientation in dye- doped nematics”, Mol. Cryst. Liq. Cryst, Vol. **251**, Issue. **1**, pp. **73**, **1994**.
- [48] Shettigar. S, Umesh. G, Chandrasekaran. K and Kalluraya. B, “Third order nonlinear optical properties and two photon absorption in newly synthesized phenyl sydnone doped polymer”, Synth. Met, Vol. **57**, Issue. **1**, pp. **142-146**, **2007**.
- [49] Vesta. C, Uthrakumar. R, Varghese. B, Mary Navis Priya. S and Jerome Das. S, “Growth, structural investigation and characterization on novel organic NLO single crystal: Trinitrophenol para hydroxyacetophene”, J. Cryst. Growth, Vol. **311**, Issue. **6**, pp. **1516-1520**, **1999**.
- [50] Zhou. YS, Wang. EB, Peng. J, Liu. J, Hu. C, Huang. R and You. X, “Synthesis and the third- order optical nonlinearities of two novel charge-transfer complexes of a heteropoly blue type (C₉H₇No)₄ H₇PMO₁₂O₄₀.3H₂O (C₉H₇No = quinolin-8-ol) and (phen)₃ H₇PMo₁₂ O₄₀. CH₃ CH₂O (phen = 1, 10-phenanthroline)”, Polyhedron, Vol. **18**, Issue. **10**, pp. **1419-1423**, **1999**.

AUTHORS PROFILE

The author of correspondence of this article
Dr. B. MILTON BOAZ Ph.D. in Physics is working as Assistant Professor in the Department of Physics, Presidency college (Autonomous) Chennai – 600 005, Tamil Nadu, India. He has 17 years of teaching experience and 19 years of research experience. He has guided 5 Ph.D. thesis and several M.Phil. and P.G. project thesis. His research interest includes Material science, Crystal Growth, Nanomaterials and Materials characterization. He has published more than 60 research papers international journals and presented more than 100 papers in international and national conferences. His research papers are cited by more than 646 international journals.